# Miocene to present kinematics of fault-bend folding across the Huerguosi anticline, northern Tianshan (China), derived from structural, seismic, and magnetostratigraphic data

Julien Charreau[1*], Jean-Philippe Avouac[1], Yan Chen[2], Stéphane Dominguez[3], Stuart Gilder[4]
[1]Tectonics Observatory, California Institute of Technology, Mail Code 100-23, Pasadena, California 91125, USA
[2]Institut des Sciences de la Terre d'Orléans, Bâtiment Géosciences, rue de Saint Amand, BP 6759, 45067 Orléans Cedex 2, France
[3]Géosciences Montpellier UMR 5243 CNRS-UMII, cc.60, Université Montpellier 2, 34095 Montpellier Cedex, France
[4]Ludwig Maximilians University, Department of Earth and Environmental Sciences, Theresienstrasse 41, 80333 Munich, Germany

## ABSTRACT

**We combine surface structural measurements, subsurface seismic imaging, and magnetostratigraphic dating to retrieve, through geometric modeling, the detailed history of fold growth and sedimentation across the Huerguosi anticline, on the northern Tianshan piedmont, taking advantage of a beautifully exposed section of growth strata. The model assumes a fault-bend folding mechanism, consistent with subsurface fold geometry. The shortening history is obtained by least-squares fitting of the measured dip angles of the growth strata. The shortening rate across the anticline is shown to have been remarkably constant: it increased only slightly from 0.84 ± 0.04 mm/yr between 10 and 4 Ma to 1.14 ± 0.02 mm/yr over the past 4 m.y. This approach also allows correcting syntectonic sedimentation rates for the effect of the fold growth and shows that the sedimentation rates in the piggyback basin increased abruptly from ~0.4 to ~0.7 mm/yr ca. 4 Ma.**

## INTRODUCTION

A number of geodetic and morphotectonic techniques are available to estimate crustal deformation over periods ranging from the coseismic time scale to tens of thousands of years. Describing quantitatively crustal deformation over the million-year time scale over which finite geological deformation develops remains a challenge of particular relevance to problems such as fault propagation, fault interactions, folding mechanisms, mountain building, or rift development. If the context is favorable, syntectonic sedimentary layers, commonly called growth strata, can provide a record of tectonic deformation over this long-term time scale (e.g., Storti and Poblet, 1997; Suppe et al., 1992), but it is often difficult to identify growth strata and interpret them quantitatively. Moreover, identifying growth strata is also important to correctly estimate regional sedimentation rates for local tectonics.

Here we describe a case example where the history of folding and thrusting across an active anticline, the Huerguosi anticline in the northern Tianshan (Fig. 1), can be recovered due to constraints on the subsurface geometry and age of pre-growth and growth strata derived from seismic imaging and magnetostratigraphy.

## TECTONIC SETTING

The Tianshan, a 2500-km-long mountain range in Central Asia, has an average elevation of 2500 m, with summits higher than 7000 m. The present topography resulted from the late Cenozoic reactivation of a Paleozoic mountain range (Burtman, 1975; Tapponnier and Molnar, 1979; Windley et al., 1990). Reactivation started ca. 23–24 Ma, and accelerated ca. 15 Ma and 11 Ma (Charreau et al., 2008; Heermance et al., 2007; Sobel et al., 2006a, 2006b; Hendrix et al., 1994). Geodetic data indicate a shortening rate across the range, at the longitude of the study area, of ~6 mm/yr (Reigber et al., 2001; Wang et al., 2001). A significant fraction of the shortening is accommodated by folding and thrusting along the southern and northern piedmonts of the range (Avouac et al., 1993; Burchfiel et al., 1999).

Our study focused on the Dushanzi-Shawan area along the northern piedmont, where two rows of active anticlines have been recognized (Avouac et al., 1993; Burchfiel et al., 1999; Molnar et al., 1994) (Fig. 1). The most frontal one along the section investigated in this study (A-A′ in Fig. 2) is the Anjihai anticline, which formed at the tip of a blind décollement. The analysis and modeling of growth strata show that north-south shortening across that Anjihai anticline started slowly ca. 7–8 Ma, and accelerated over the last 1 m.y. from ~0.1 to ~1.1 mm/yr (Daëron et al., 2007). The Huerguosi anticline, which is the focus of this study, is a more mature structure that evolved into a fault-bend fold, with the thrust ramp breaking through the surface and offsetting Holocene river terraces (Avouac et al., 1993) (Fig. 2).

## STRUCTURE OF THE HUERGUOSI ANTICLINE

The Jingou He River has exposed a continuous section of south-dipping late Cenozoic continental strata. These include, from bottom to top, the Anjihaihe, Shawan, Taxihe, Dushanzi, and Xiyu Formations (Bureau of Geological and Mineral Resources of the Xinjiang Uygur Autonomous Region, 1985). These formations are all continental clastic, grading upward from mudstone and siltstone to the coarse conglomerate of the diachronous Xiyu Formation (Charreau et al., 2008). Deposition ages are well constrained from dense magnetostratigraphy (Charreau et al., 2008), and range from ca. 23.6 Ma to ca. 1 Ma (Fig. 2).

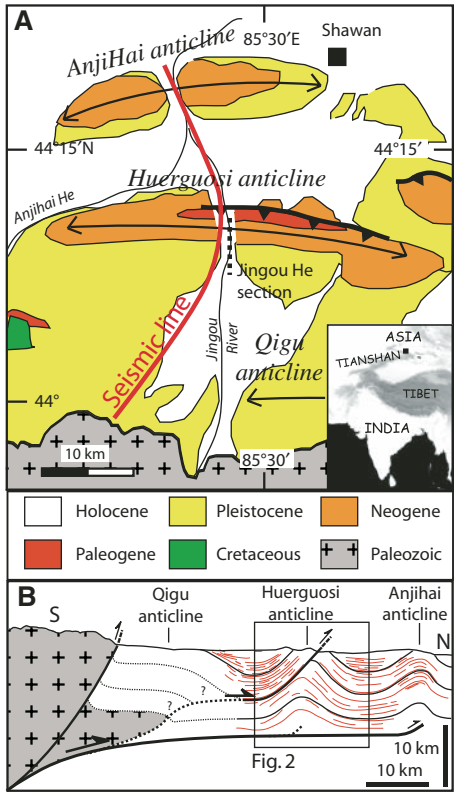


**Figure 1. A: Geological map of northern Tianshan piedmont with locations of Huerguosi, Anjihai, and Qigu anticlines, magnetostratigraphic study (dashed line) (Charreau et al., 2008), and seismic profile (He et al., 2005). B: Cross section derived from seismic profile (line drawing interpretation shown by red lines). No vertical exaggeration.**

*E-mail: jcharrea@gps.caltech.edu

To constrain the fold geometry, we measured the bedding attitude at 148 sites along the section, located with a real-time kinematic global positioning system. Strikes are fairly uniform, showing a nearly cylindrical fold structure striking ~N85°E on average. Dip angles are constant, ~55°S over a distance of ~4–5 km south of where the Huerguosi fault breaks the surface. Farther south, dip angles shallow gradually to near horizontal (Fig. 2).

The deep structure of the hanging wall, as revealed by a seismic line along the Jingou He River (GSA Data Repository Fig. DR1[1]; He et al., 2005), is consistent with a simple fault-bend fold model (Suppe, 1983) (Fig. 2; Fig. DR1). The deeper reflectors show no significant bed thickness variations and can be assumed to parallel a curved fault ramping up from a subhorizontal décollement at a depth of ~7.8 km. The dip angles measured at the surface along the few kilometers south of the fault are consistent with those predicted from the deep fold structure and the fault-bend fold model (as indicated by the dashed lines in Fig. 2), and thus indicate that these pre-growth layers were deposited either before the onset of folding or far away from the zone of active folding. Farther south, dip angles are shallower than expected for pre-growth strata, suggesting that these layers are growth strata that have recorded a fraction of the history of folding (Fig. 2).

The seismic profile also reveals a footwall anticline beneath the ramp (Figs. 1 and 2). The geometry of this anticline is typical of a fault-tip fold, like the Anjihai anticline located to the north (Fig. 1) (Daëron et al., 2007). Following a scenario initially deduced from the analysis of structural sections across other anticlines along the northern Tianshan piedmont (Avouac et al., 1993), we interpret it as a relict of the early phase of development of the Huerguosi anticline: the early anticline was preserved in the footwall as the fold evolved toward a fault-bend fold when the ramp broke behind the initially formed fault-tip fold.

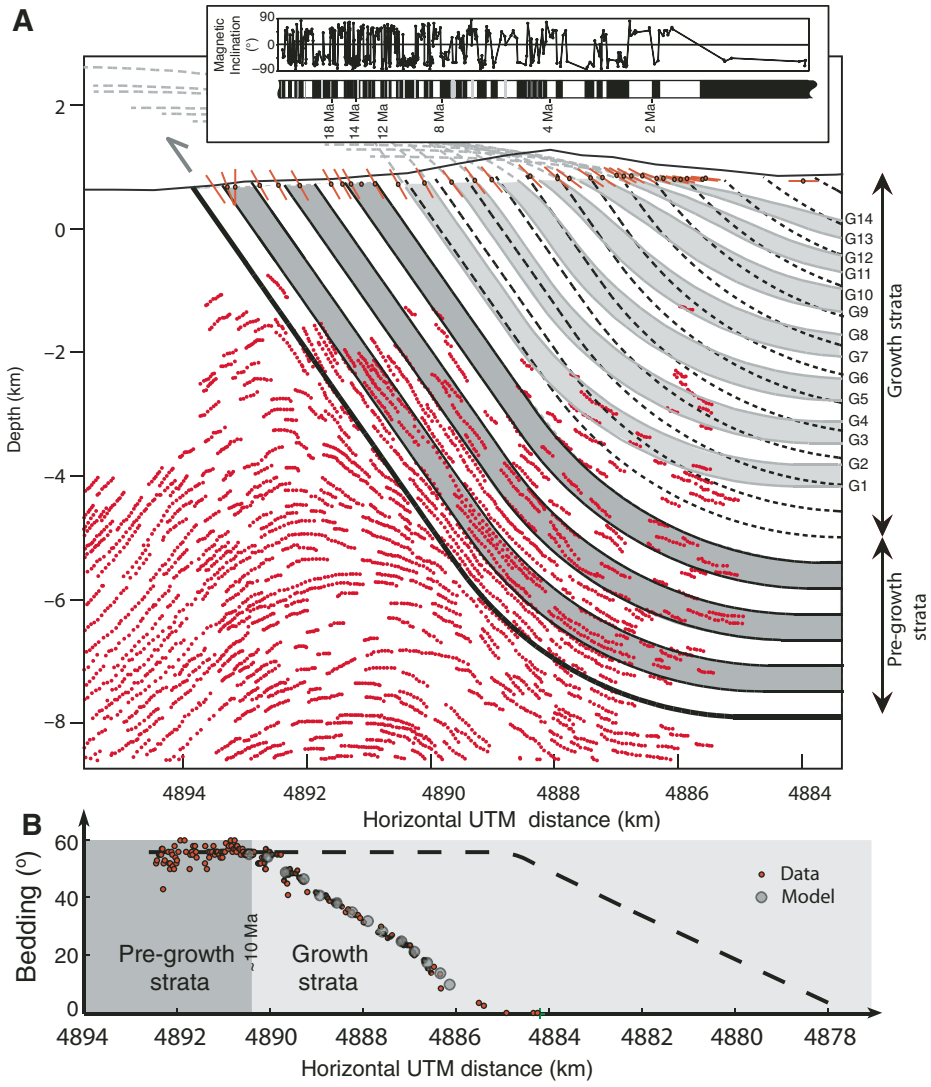


**Figure 2. A: Line drawing of seismic profile across Huerguosi anticline (He et al., 2005), and measured dip angles along Jingou He River. Traveltimes were converted to depth assuming uniform velocity of ~2900 m/s so as to obtain shallow reflectors within the hanging wall parallel to beds measured at surface. Pre-growth (black continuous and dashed line), and growth (continuous gray line) strata predicted by fault-bend folding are also shown. Measured magnetic inclinations and inferred chronology are at top. B: Measured (red dot) and predicted (continuous line or gray dots) dip angles from fault-bend folding, assuming curved fold and finite width hinge. Dashed line shows dip angles predicted by fault-bend folding for pre-growth strata. Sediments deposited south of 4891.5 km are clearly growth strata. UTM—Universal Transverse Mercator.**

## FORWARD MODELING AND SHORTENING HISTORY ACROSS HUERGUOSI ANTICLINE

The onset of the development of the growth strata is estimated to be ca. 9–10 Ma; thanks to the high-resolution chronology provided by the magnetostratigraphy (Charreau et al., 2008), a detailed history of shortening across the Huerguosi anticline can be derived. To do so, we model the fold structure assuming a fault-bend fold model in which only bed-parallel shear is allowed (Suppe, 1983). Following Suppe et al. (1997) and Hubert-Ferrari et al. (2007), we consider an axial surface of finite width limited by entry and exit axial surfaces that bound a curved fold (Fig. DR2). In such a setting, the depositional pattern then reflects the hinge zone migration within the hanging wall. The trajectory of any point during folding corresponding to a shortening $S$ can be computed from the equations in Appendix DR1. The key parameters are the radius of curvature of the hinge zone, $Rc$ = 5600 m, and the opening angle of the curved fold, $\beta = 55°$, which are determined from the geometry of pre-growth strata at depth (Fig. 2).

We consider 14 growth-strata layers ($G_1$ to $G_{14}$ in Fig. 2) initially deposited horizontally across the Huerguosi fold at a given elevation above the décollement ($Z_1$ to $Z_{14}$), each assumed to have undergone a varying amount of shortening ($S_1$ to $S_{14}$). The effect of compaction is ignored in the modeling but can be corrected for (see Appendix DR4). For each layer, $S_i$ is determined by least-squares adjustment between the observed dip angles, $\theta_{obs}$ and the modeled dip angles, $\theta_{mod}$ (see Appendix DR2 for the calculation of uncertainties). The age of each modeled layer

[1]GSA Data Repository item 2008223, Appendices DR1-DR4, and Figures DR1 and DR2 (kinematic model, calculation of uncertainties and shortening rates, and compaction effect), is available online at www.geosociety.org/pubs/ft2008.htm, or on request from editing@geosociety.org or Documents Secretary, GSA, P.O. Box 9140, Boulder, CO 80301, USA.

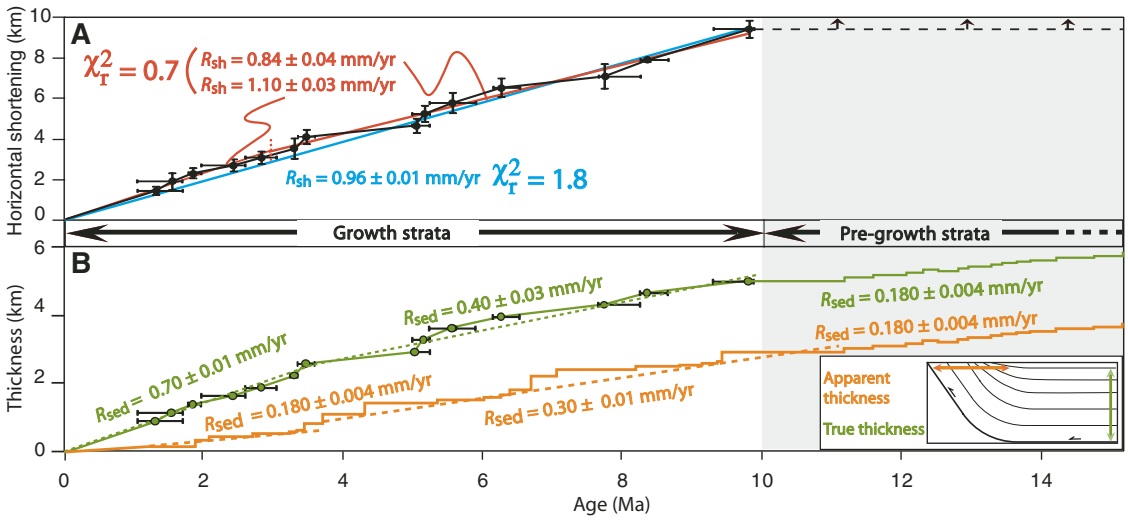


**Figure 3. A: Inferred time evolution of shortening (black line and symbols) across Huerguosi anticline. Blue line shows best least-squares fit to data assuming constant shortening rate over past 10 m.y. Red line shows best linear fit assuming two periods of constant shortening rate. Age of the transition between the two periods was adjusted so as to maximize the fit to data. Data fitting procedure is detailed in Appendix DR3 (see footnote 1). B: Time evolution of sedimentation during deposition of growth strata (orange line). Green line shows estimated sedimentation history in the piggyback basin, where it is not diminished by fold growth rate. $R_{sed}$—sedimentation rates derived from least-squares linear fit (dashed lines).**

($t_1$ to $t_{14}$) was estimated by linear interpolation of the ages derived from the magnetostratigraphic study assuming a constant sedimentation rate within each chron (see Appendix DR3 for the calculation of uncertainties). Uncertainties on shortening values account for dip angle measurement errors, but ignore uncertainties on the model geometry or on the validity of the bed-parallel shear assumption.

While our model was constrained from surface measurements only, it also reproduces remarkably well the geometry of seismic reflectors within the pre-growth strata (Fig. 2). This shows that the model is probably appropriate.

## DISCUSSION

### Development of the Huerguosi Anticline

Strata older than ca. 10 Ma are clearly pre-growth strata and underwent a minimum shortening of ~9425 m. Folding may have started earlier, but there is no direct record left in the hanging wall. The earlier history of the fold is probably recorded in the footwall anticline, which reveals that it probably developed initially as a fault-tip fold, like the Anjihai anticline (Daëron et al., 2007). Later a ramp broke through the sedimentary cover behind the footwall anticline and the fold evolved as a fault-bend fold. The monoclinal dips of the pre-growth strata both in the seismic profile and at the surface suggest that the ramp thrust is nearly linear and has not been affected by the growth of the underlying footwall anticline. This likely indicates that the footwall anticline stopped being active when the ramp formed. Also, because our model predicts surface dip angles as well at the subsurface geometry, it is probable that the growth strata were entirely associated with the fault-bend folding phase. Furthermore, the succession of an early phase of fault-tip folding and later phase of fault-bend folding is also observed in analogue experiments (e.g., Bernard et al., 2007). Despite that, our analysis does not bring much constraint on the onset of formation of the footwall anticline; by analogy with the Anjihai anticline model, it is possible that the footwall anticline developed over a very long period of time at a relatively slow pace.

### Shortening History Across Huergueosi Anticline and Interaction with Anjihai Anticline

The growth strata show that over the past 10 m.y., slip on the Huerguosi thrust fault has absorbed a nearly constant shortening rate, estimated to be 0.96 ± 0.01 mm/yr (at the 67% confidence level). This rate was calculated by adjusting the shortening-time data set in Figure 3 from a straight-line $S = R_{sh} \cdot t$ (see Appendix DR3 for details). The data suggest a somewhat larger shortening rate ($R_{sh}$) after ca. 4 Ma and a slower one before. If we now assume a different shortening rate for these two periods, we get a rate of 1.14 ± 0.02 mm/yr from 0 to ca. 4 Ma and 0.84 ± 0.04 mm/yr from 4 to ca. 10 Ma. From an F-test, the probability that the two periods have the same rate is <1%. So, although the data show only slight temporal variations of shortening rates, it seems that these variations are significant in view of the estimated uncertainties (Appendix DR3).

It is interesting to note that the estimate from 0 to 4 Ma is rather coherent with Holocene rates of ~1.3 mm/yr deduced from the vertical throw rate of 1.1 mm/yr determined from offset terraces whose ages were estimated from morphologic dating (Avouac et al., 1993), and the 55° fault dip angle.

The Anjihai and Huerguosi anticlines probably both root in the same décollement, and their histories reveal how they have contributed to absorb thrusting at the front of the northern Tianshan piedmont (Fig. 1). Some fraction of the shortening across the piedmont is missing, however, because the Qigu anticline has also probably been active over this period of time (Burchfiel et al., 1999) (Fig. 1), and the shortening accommodated by the fault-tip fold in the footwall of the Huerguosi thrust fault is ignored. Nonetheless, it is clear that deformation had started by ca. 10 Ma and that the shortening rate across the piedmont was a minimum of 0.84 mm/yr at the time. It increased to at least 1.24 mm/yr when the Anjihai anticline became active, increased to ~1.5 mm/yr when the slip rate on the Huerguosi thrust fault increased ca. 4 Ma, and increased to ~2.2 mm/yr over the past ~1 m.y.

These shortening rates are comparable to the shortening rate across the nearby Dushanzi anticline, the main active structure across the piedmont just east of our study area, estimated at between 1 and 5 mm/yr over the Quaternary and Holocene (Burchfiel et al., 1999; Molnar et al., 1994; Poisson and Avouac, 2004).

### Interaction Between Fold Growth and Sedimentation

The pre-growth strata indicate sedimentation rates (not corrected for compaction) of 0.18 mm/yr on average between 15–16 and 10–11 Ma (Charreau et al., 2008). The sedimentation rate within the growth strata (red curve in Fig. 3) can be corrected for the fold growth, using our kinematic fold model, to estimate the sedimentation rate in the piggyback basin (blue curve in Fig. 3). If the effect of the fold growth is taken into account, the picture is significantly modified. It shows an amplified increase in sedimentation rate ca. 10 Ma, first identified in the complete magnetostratigraphic section

(Charreau et al., 2008), from ~0.2 mm/yr to 0.4 mm/yr, and an even more obvious increase from 0.4 to 0.7 mm/yr ca. 4 Ma.

The coeval increase of sedimentation rate and shortening rate would suggest a causal relationship, probably because the growing topography of the anticline may have contributed to trapping sediments in the piggyback basin. However, similar and coeval increases of sedimentation rate ca. 10 Ma are observed in a number of different sections across the northern and southern piedmont of the Tianshan (Charreau et al., 2006; Heermance et al., 2007). It is therefore more probable that this increase reflects a regional effect rather than a local cause. The 0.26 mm/yr increase of shortening rate ca. 4 Ma seems too small (it corresponds to a 0.2 mm/yr increase of uplift rate) for this trapping process to explain entirely the 0.3 mm/yr increase in sedimentation rate ca. 4 Ma. Therefore, this increase may reflect a more regional effect, for example related to global climate cooling described for 2–4 Ma (Zhang et al., 2001).

## CONCLUSION

This study demonstrates how subsurface imaging, precise magnetostratigraphic dating of pre-growth and growth strata, and simple structural models of fold development can be combined to retrieve a fold history and sedimentation rates with accuracy. This is a powerful approach to study the development of fold-and-thrust belts at the fronts of active mountain ranges, and investigate the mechanics of fault-related folding and fault interactions. This study also demonstrates that sedimentation rate profiles derived from magnetostratigraphic sections must be interpreted with caution, because local tectonic effects can lead to sedimentation rates either lower or larger than the regional rates, depending on whether deposition occurred within the piggyback or in the section affected by folding. In any case the kind of modeling described here offers a way to assess quantitatively these effects.


## ACKNOWLEDGMENTS

We thank Ed Sobel and Aurelia Hubert-Ferrari for helpful reviews. We are also grateful to Sebastien Leprince and Mathieu Daëron for fruitful discussions and help in the statistical analysis. This study was financed by the Institut National des Sciences de l'Univers French program ECLIPSE, the Agence National pour la Recherche, and the Gordon and Betty Moore Foundation. This is Caltech Tectonics Observatory contribution 89.


## REFERENCES CITED


Avouac, J.-P., Tapponnier, P., Bai, P., You, M., and Wang, G.A., 1993, Active thrusting and folding along the northern Tien Shan and late Cenozoic rotation of the Tarim relative to Dzungaria and Kazakhstan: Journal of Geophysical Research, v. 98, p. 11,791–11,808.

Bernard, S., Avouac, J.P., Dominguez, S., and Simoes, M., 2007, Kinematics of fault-related folding derived from sandbox experiment: Journal of Geophysical Research, v. 112, B03S12, doi: 10.129/2005JB0044149.

Burchfiel, B.C., Brown, E.T., Qidong, D., Li, J., Feng, X., Molnar, P., Shi, J., Wu, Z., and You, H., 1999, Crustal shortening on the margins of the Tian Shan, Xinjiang, China: International Geology Review, v. 41, p. 663–700.

Bureau of Geological and Mineral Resources of the Xinjiang Uygur Autonomous Region, 1985, Geological map of the Xinjiang Uygur Autonomous Region, China: Beijing, China Geological Printing House.

Burtman, V.S., 1975, Structural geology of the Variscan Tian Shan, USSR: American Journal of Science, v. 275-A, p. 157–186.

Charreau, J., Gilder, S., Chen, Y., Dominguez, S., Avouac, J.-P., Sevket, S., Jolivet, M., Li, Y., and Wang, W., 2006, Magnetostratigraphy of the Yaha section, Tarim Basin (China): 11 Ma acceleration in erosion and uplift of the Tian Shan Mountains: Geology, v. 34, p. 181–184.

Charreau, J., Chen, Y., Gilder, S., Barrier, L., Dominguez, S., Augier, R., Sen, S., Avouac, J.-P., Gallaud, A., Graveleau, F., and Li, Y., 2008, Neogene uplift pulses of the Tianshan mountains observed in the magnetic record of the Jingou River section (Northwest China): Tectonics (in press).

Daëron, M., Avouac, J.-P., Charreau, J., and Dominguez, S., 2007, Modeling the shortening history of a fault-tip fold using structural and geomorphic records of deformation: Journal of Geophysical Research, v. 12, B03S13, doi: 10.1029/2006JB004460.

He, D., Suppe, J., Geng, Y., Shuwei, G., Shaoying, H., Xin, S., Xiaobo, W., and Chaojun, Z., 2005, Guide book for the field trip in south and north Tianshan foreland basin, Xinjiang Uygur Autonomous Region, China, International conference on theory and application of fault-related folding in foreland basins: Beijing, China Geological Printing House, 77 p.

Heermance, R.V., Chen, J., Burbank, D.W., and Wang, C., 2007, Chronology and tectonic controls of late Tertiary deposition in the southwestern Tian Shan foreland, NW China: Basin Research, v. 19, p. 599–632, doi: 10.1111/j.1365–2117.2007.00339.x.

Hendrix, M.S., Dumitru, T.A., and Graham, A.S., 1994, Late Oligocene–early Miocene unroofing in the Chinese Tian Shan: An early effect of the India-Asia collision: Geology, v. 22, p. 487–490.

Hubert-Ferrari, A., Suppe, J., Gonzalez-Mieres, R., and Wang, X., 2007, Mechanism of active folding of the landscape (southern Tian Shan, China): Journal of Geophysical Research, v. 112, B03S09, doi: 10.129/2006JB004362.

Molnar, P., Brown, E.T., Burchfiel, B.C., Deng, Q., Feng, X., Li, J., Raisbeck, G.M., Shi, J., Wu, Z., Yiou, F., and You, H., 1994, Quaternary climate change and the formation of river terraces across growing anticlines on the north flank of the Tien Shan, China: Journal of Geology, v. 102, p. 583–602.

Poisson, B., and Avouac, J.-P., 2004, Holocene hydrological changes inferred from alluvial stream entrenchment in North Tian Shan (northwestern China): Journal of Geology, v. 112, p. 231–249, doi: 10.1086/381659.

Reigber, C., Michel, G.W., Galas, R., Angermann, D., Klotz, J., Chen, J.Y., Papschev, A., Arslanov, R., Tzurkov, V.E., and Ishanov, M.C., 2001, New space geodetic constraints on the distribution of deformation in the Central Asia: Earth and Planetary Science Letters, v. 191, p. 157–165, doi: 10.1016/S0012–821X(01)00414–9.

Sobel, E.R., Oskin, M., Burbank, D., and Mikolaichuk, A.V., 2006a, Exhumation of basement-cored uplifts: Example of the Kyrgyz Range quantified with apatite fission track thermochronology: Tectonics, v. 25, TC2008, doi: 10.1029/2005TC001809.

Sobel, E., Chen, J., and Heermance, R.V., 2006b, Late Oligocene–early Miocene initiation of shortening in the Southwestern Chinese Tian Shan: Implications for Neogene shortening rate variations: Earth and Planetary Science Letters, v. 247, p. 70–81.

Storti, F., and Poblet, J., 1997, Growth stratal architectures associated to decollement folds and fault-propagation folds. Inferences on fold kinematics: Tectonophysics, v. 282, p. 353–373, doi: 10.1016/S0040–1951(97)00230–8.

Suppe, J., 1983, Geometry and kinematics of fault-bend folding: American Journal of Science, v. 283, p. 684–721.

Suppe, J., Chou, G.T., and Hook, S.C., 1992, Rates of folding and faulting determined from growth strata, *in* McClay, K.R., ed., Thrust tectonics: New York, Chapman and Hall, p. 105–121.

Suppe, J., Sabat, F., Munoz, J.A., Poblet, J., Roca, E., and Verges, J., 1997, Bed-by-bed fold growth by kink-band migration; Sant Llorenc de Morunys, eastern Pyrenees: Journal of Structural Geology, v. 19, p. 443–461, doi: 10.1016/S0191–8141(96)00103–4.

Tapponnier, P., and Molnar, P., 1979, Active faulting and Cenozoic tectonics of the Tien Shan, Mongolia, and Baykal regions: Journal of Geophysical Research, v. 84, p. 3425–3459, doi: 10.1029/JB084iB07p03425.

Wang, Q., Zhang, P.-Z., Freymueller, J.T., Bilham, R., Larson, K.M., Lai, X., You, X.Z., Niu, Z.J., Wu, J.C., Li, Y.X., Liu, J.N., Yang, Z.Q., and Chen, Q.Z., 2001, Present-day crustal deformation in China constrained by global positioning system measurements: Science, v. 294, p. 574–577, doi: 10.1126/science.1063647.

Windley, B.F., Allen, M.B., Zhang, C., Zhao, Z.-Y., and Wang, G.R., 1990, Paleozoic accretion and Cenozoic redeformation of the Chinese Tien Shan Range, Central Asia: Geology, v. 18, p. 128–131, doi: 10.1130/0091–7613(1990)018<0128:PAACRO>2.3.CO;2.

Zhang, P., Molnar, P., and Downs, W.R., 2001, Increased sedimentation rates and grain sizes 2–4 m.y. ago due to the influence of climate change on erosion rates: Nature, v. 410, p. 891–897.



Manuscript received 3 May 2008
Revised manuscript received 28 July 2008
Manuscript accepted 28 July 2008

Printed in USA